

# Synthesis, crystal structure and nonlinear optical property of $\text{CsV}_2\text{O}_5$

Hong Luo, Jianguo Pan\*, Bingqian Lou, Yuebao Li, Xing Li, Lei Han

State Key Laboratory Base of Novel Functional Materials and Preparation Science, Faculty of Materials Science and Engineering, Ningbo University, Ningbo, Zhejiang 315211, PR China

## ARTICLE INFO

### Article history:

Received 23 August 2012

Accepted 18 October 2012

Available online 26 October 2012

### Keywords:

Crystal structure

Nonlinear optical material

$\text{CsV}_2\text{O}_5$

## ABSTRACT

The new nonlinear optical crystal  $\text{CsV}_2\text{O}_5$  has been synthesized by solid state reaction and characterized by single-crystal X-ray diffraction and thermogravimetric analysis. The crystal  $\text{CsV}_2\text{O}_5$  crystallizes in the orthorhombic system with space *Ima2* space group. It is a layered structure that is very flat and strongly parallel to *c*. The striking structural feature is that the V atom in single crystallographic site has two different valence states ( $\text{V}^{4+}$  and  $\text{V}^{5+}$ ). The  $[\text{V}_2\text{O}_5]_n$  layer consists of corner-linked tetrahedron. The six tetrahedrons lie very nearly in the same *z*-plane forming almost regular hexagons. The Kurtz powder SHG measurement, using 1064 nm radiation, showed that the second-harmonic generation efficiency of  $\text{CsV}_2\text{O}_5$  is about six times that of KDP.

© 2012 Elsevier B.V. All rights reserved.

During the past two decades, the design and characterization study of second-order nonlinear optical (NLO) materials have become a hotspot for a lot of chemistry and physics scholars due to their wide commercial applications in laser frequency conversion, optical parameter oscillators, Q-switch signal processing and information storage [1,2]. Great progress has been made in searching for novel NLO crystals in inorganic oxides, organic crystals, polymers and organometallic compounds [3–5]. In general, vanadium may exist as  $\text{V}^0$  (metallic),  $\text{V}^{2+}$ ,  $\text{V}^{3+}$ ,  $\text{V}^{4+}$  and  $\text{V}^{5+}$  depending on the synthesis procedure and chemical environment. Therefore, it can be the formation of many new structures, and has many interesting properties. Our interest in vanadium is based on its ability to form distorted tetrahedron, pentahedron, triangular pyramids, and octahedron. This type of distortion is prevalent in high-valent, *d*<sup>0</sup> transition metals owing to the symmetry-allowed mixing of a low-lying excited state (LUMO) with a nondegenerate ground-state molecular orbital (HOMO) [6–8]. This orbital mixing results in a distortion of the geometry of the metal centers along the C2, C3, or C4 axes [9,10]. Based on the above the new polar solids with large second-harmonic generation (SHG) responses can be prepared by combining distorted pentavanadium oxygen polyhedron and a large counterion, such as  $\text{ACa}_9(\text{VO}_4)_7$  [11],  $\text{Ba}_{1.5}\text{VOSi}_2\text{O}_7$  [12],  $\text{K}_3\text{V}_5\text{O}_{14}$  [13],  $\text{Rb}_3\text{V}_5\text{O}_{14}$  [14], and  $\text{A}[(\text{VO})_2(\text{IO}_3)_3\text{O}_2]$  ( $\text{A} = \text{NH}_4^+$ , Rb, Cs) [15], which are of interest as a result of their nonlinear optical properties as well as their piezoelectric and pyroelectric properties.

The compound  $\text{CsV}_2\text{O}_5$  with space group  $\text{P}_{21/c}$  was reported and synthesized by two methods. The first kind is electrolysis of  $\text{Cs}_2\text{O}$  and  $\text{V}_2\text{O}_5$  melt at high temperature [16], the second is the solid-state reaction of mixtures with appropriate molar ratios of  $\text{CsVO}_3$ ,  $\text{V}_2\text{O}_3$  and  $\text{V}_2\text{O}_5$  in an evacuated silica tube [17]. It was a

centrosymmetric structure and has no second-harmonic generation (SHG) responses. In this paper, we report the synthesis, structure, and nonlinear optical properties of a new isomorphous phase of  $\text{CsV}_2\text{O}_5$ .

The brown single crystals of  $\text{CsV}_2\text{O}_5$  were obtained by high-temperature solid-state reaction. The stoichiometric amounts of  $\text{Cs}_2\text{CO}_3$ (AR) and  $\text{V}_2\text{O}_5$ (AR) were weighed accurately. These mixtures were pressed into tablets and then placed in platinum crucible. Platinum was selected since it is essentially chemically inert in this system. The samples were gradually heated to 500°C for 15 h, held for 120 h, and then allowed to cool to about 100°C at a controlled temperature reducing rate of 10°C/h in the furnace in carbon monoxide atmosphere. Isomorphous phases of  $\text{AV}_2\text{O}_5$  ( $\text{A} = \text{Na}$ , K, Rb) were not obtained by the same method.

Single-crystal X-ray diffraction analysis [18] revealed that  $\text{CsV}_2\text{O}_5$  crystallizes in the *Ima2* space group [Table S1.S2] and displays a two-dimensional layer structure separated by Cs<sup>+</sup> cations (Fig. 1a). The EPR spectrum at 293 K (Fig. S1) shows  $\text{V}^{4+}$  signal with  $g = 1.95$ , suggesting that the synthesized sample is mixed-valence compounds. The calculated total bond valence for V is 4.528. This indicates that the V atoms are in an oxidation state of +4.5, and confirms that V site is really mixed-valent. The striking structural feature is that the V atom in single crystallographic site has two different valence states ( $\text{V}^{4+}$  and  $\text{V}^{5+}$ ). The layer character of this structure is very flat and strongly parallel to *c*. The  $[\text{V}_2\text{O}_5]_n$  layer consists of corner-linked tetrahedron. As will be seen, the V atoms form four different bonds with  $\text{O}_1$ ,  $\text{O}_2$ ,  $\text{O}_3$ , and  $\text{O}_4$  atoms, and form distorted tetrahedrons, V–O bond distances and O–V–O angles for tetrahedron are listed in table [S3.S4]. The tetrahedrons with apices pointing in the same direction along the *c*-axis are joined by sharing neighboring basal corners. The six tetrahedrons lie very nearly in the same *z*-plane forming almost regular hexagons (Fig. 1b). The tetrahedral sublattice was equally occupied by  $\text{V}^{4+}$  and  $\text{V}^{5+}$ . Each hollow space resulting from the six-ring configuration is occupied by a rubidium atom, placed

\* Corresponding author. Tel.: +86 574 7600793; fax: +86 574 87600734.

E-mail address: [panjianguo@nbu.edu.cn](mailto:panjianguo@nbu.edu.cn) (J. Pan).

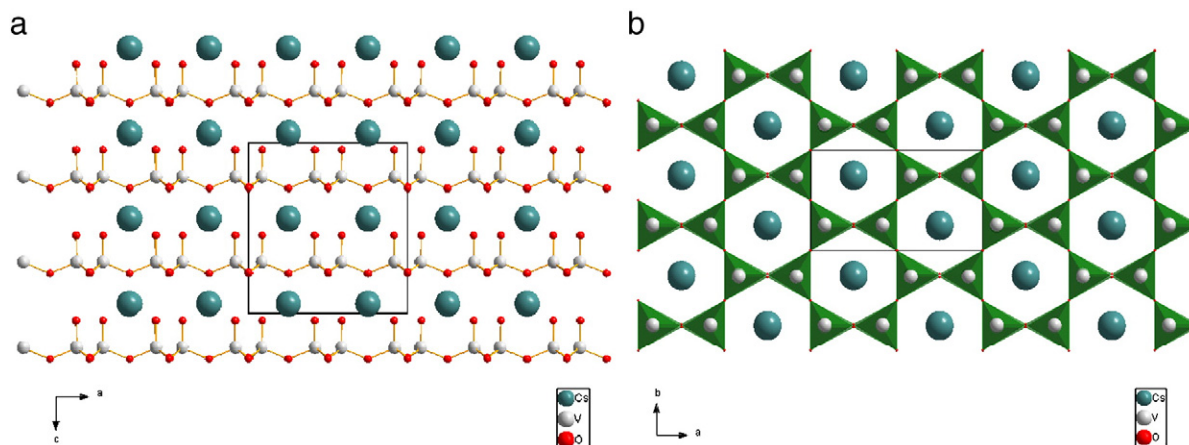


**Fig. 1.** View of the structure of  $\text{CsV}_2\text{O}_5$ , corner-connected  $\text{VO}_4$  triangular pyramids interspersed with layers Cs ions (the green balls) is shown in projection down the  $[010]$  direction in (a) and the  $[001]$  direction in (b).

about half way between the layers. The interstitial Cs atom is nominally surrounded by 12 oxygens, six oxygens from the apex oxygen's of the tetrahedrons in the lower layer and six oxygens from basal corner of tetrahedrons in the layer above. This packing mode is favorable to the accumulation of microscopic second-order NLO coefficient and exhibits a relatively strong bulk NLO effect.

The experimental powdered X-ray diffraction (XRD) pattern of  $\text{CsV}_2\text{O}_5$  agrees well with the simulated one based on the single-crystal X-ray data (Fig. 2), indicating that the sample of  $\text{CsV}_2\text{O}_5$  is in a pure phase. But the diffraction intensity has some difference compared to the indexed and simulation pattern due to many factors such as the size of powder particulate, the control of the scanning conditions and the crystalline degree.

Thermogravimetric analysis (Fig. 3) shows that  $\text{CsV}_2\text{O}_5$  can be thermally stable up to  $700^\circ\text{C}$ , and there isn't weight loss. The heating and the cooling DTA curves of  $\text{CsV}_2\text{O}_5$  crystal show that crystal  $\text{CsV}_2\text{O}_5$  melts congruently (Fig. 3). The melting point of the crystal is about  $450^\circ\text{C}$ , the  $\text{CsV}_2\text{O}_5$  material begins to freeze about  $410^\circ\text{C}$ .

A preliminary SHG efficiency measurement of  $\text{CsV}_2\text{O}_5$  has been carried out by the Kurtz–Perry method using polycrystalline samples at room temperature. In addition to identifying the materials with noncentrosymmetric crystal structure, it is also used as a screening

technique to identify the materials with the capacity for phase matching. The SHG intensity from the material is measured as a function of particle size. The continuous increase of SHG intensity with increasing of particle size confirms the phase matching behavior of the material. An inverse relation between intensity and particle size confirms the non-phase matching behavior of the material.

With the  $100\ \mu\text{m}$  particle size, the intensity of the green light (frequency-doubled output:  $\lambda = 532\ \text{nm}$ ) produced by the  $\text{CsV}_2\text{O}_5$  powder is about six times that of KDP powder, indicating that  $\text{CsV}_2\text{O}_5$  six times the SHG efficiency of KDP. The curves (Fig. 4) of SHG signal as a function of particle size have been obtained, which are not consistent with phase-matching behavior. The continuous decrease of SHG with increasing of particle size [22,23] shows that  $\text{CsV}_2\text{O}_5$  crystal is non-phase matching behavior.

In summary, a novel second-order NLO material of Cesium pentavanadium was synthesized by high-temperature solid-state reaction. The crystal  $\text{CsV}_2\text{O}_5$  crystallizes in the orthorhombic system with  $\text{Ima}2$  space group, namely a noncentrosymmetric (NCS) structure. The four O anions form the distorted tetrahedrons which lie very nearly in the same  $z$ -plane forming almost regular hexagons. This packing mode is favorable to the accumulation of microscopic second-order NLO coefficient and exhibits a relatively strong bulk NLO effect. The intensity of second harmonic generation effect is about six times as large as that of KDP. The melting point of  $\text{CsV}_2\text{O}_5$  is about  $398^\circ\text{C}$ . It is possible for  $\text{CsV}_2\text{O}_5$  to possess potential application as a new NLO crystal.

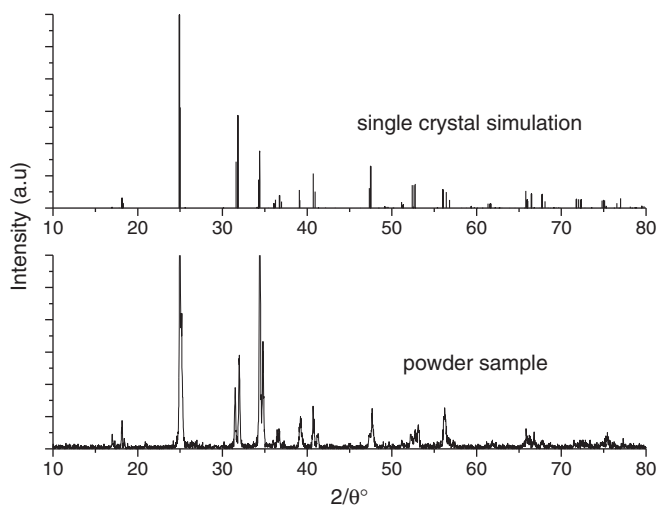


**Fig. 2.** The pattern of X-ray powder diffraction: (a) single crystal simulation pattern, and (b) powder sample pattern.

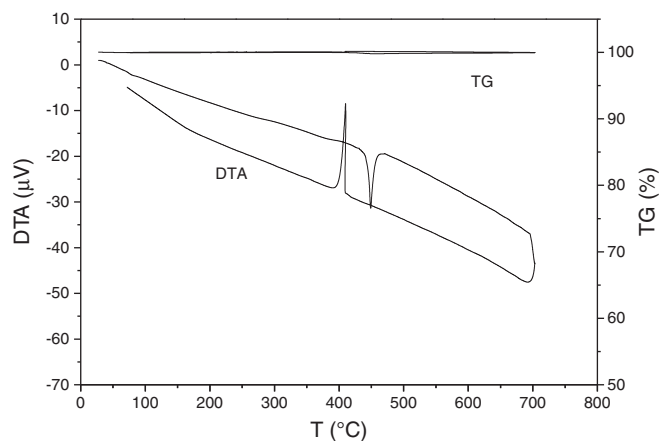


**Fig. 3.** TG and DTA curves of  $\text{CsV}_2\text{O}_5$  crystal.

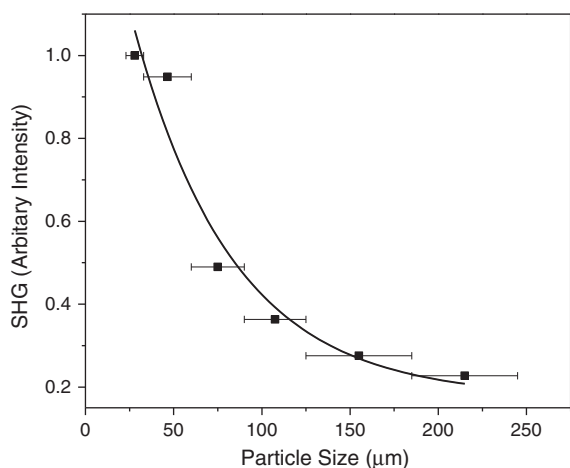


Fig. 4. Particle-size dependence of second-harmonic intensity for  $\text{CsV}_2\text{O}_5$  powders. (The black curve is a fitting curve).

### Acknowledgments

This work is partially supported by the National Natural Science Foundation of China (No. 61078055), the program of Key Team of Technological Innovation of Zhejiang Province (Grant 2011R09025-01), Foundation of Ningbo University (zj1120, xk1067) and the K.C.Wang magna Fund in Ningbo University.

### Appendix A. Supplementary data

Supplementary data to this article can be found online at <http://dx.doi.org/10.1016/j.inoche.2012.10.023>.

### References

- [1] S.B. Lang, D.K. Das-Gupta, in: H.S. Nalwa (Ed.), *Handbook of Advanced Electronic and Photonic Materials and Devices*, vol. 4, Academic Press, San Francisco, 2001, pp. 1–55.
- [2] C. Chen, G. Liu, Recent advances in nonlinear optical and electro-optical materials, *Annu. Rev. Mater. Sci.* 16 (1986) 203–243.
- [3] C.-F. Sun, C.-L. Hu, X. Xu, B.-P. Yang, J.-G. Mao, Explorations of new second-order nonlinear optical materials in the potassium vanadyl iodate system, *J. Am. Chem. Soc.* 133 (2011) 5561–5572.
- [4] P. Becker, Borate materials in nonlinear optics, *Adv. Mater.* 10 (1998) 979–992.
- [5] Jian-Gong Pan, Gong-Jun Zhang, Yue-Qing Zheng, Jian-Li Lin, Wei Xu, Growth and characterization of a novel nonlinear optical crystal zinc succinate,  $\text{Zn}(\text{C}_4\text{H}_4\text{O}_4)$ , *J. Cryst. Growth* 308 (1) (2007) 89–92.
- [6] R.A. Wheeler, M.H. Whangbo, T. Hughbanks, R. Hoffman, J.K. Burdett, T.A. Albright, Symmetric vs. asymmetric linear M–X–M linkages in molecules, polymers, and extended networks, *J. Am. Chem. Soc.* 108 (1986) 2222–2236.
- [7] S.K. Kang, H. Tang, T.A. Albright, Structures for  $\text{d}0 \text{ML}_6$  and  $\text{ML}_5$  complexes, *J. Am. Chem. Soc.* 115 (1993) 1971–1981.
- [8] R.E. Cohen, Origin of ferroelectricity in perovskite oxides, *Nature* 358 (1992) 136–138.
- [9] M. Kunz, I.D. Brown, Out-of-center distortions around octahedrally coordinated  $\text{d}0$  transition metals, *J. Solid State Chem.* 115 (1995) 395–406.
- [10] J.B. Goodenough, J.M. Longo, Crystallographic and magnetic properties of perovskite and perovskite-related compounds, in: K.H. Hellwege, A.M. Hellwege (Eds.), *Landolt-Bornstein*, 4, Springer-Verlag, Berlin, 1970, pp. 126–314.
- [11] J.S.O. Evans, J. Huang, A.W. Sleight, Synthesis and structure of  $\text{ACa}_9(\text{VO}_4)_7$  compounds, A = Bi or a rare Earth, *J. Solid State Chem.* 157 (2001) 255–260.
- [12] K. Ramesha, J. Gopalakrishnan, Chimie douce synthesis of a new nonlinear optical material:  $\text{Ba}_{1.5}\text{VO}_5\text{O}_7$ , *Solid State Sci.* 3 (2001) 113–119.
- [13] G. Li, G. Su, X. Zhuang, Z. Li, Y. He, Characterization and properties of a new IR nonlinear optical crystal:  $\text{K}_3\text{V}_5\text{O}_{14}$ , *Opt. Mater.* 27 (2004) 539–542.
- [14] Jianguo Pan, Yuebao Li, Yuejie Cui, Lingyan Zhao, Xing Li, Lei Han, Synthesis, crystal structure and nonlinear optical property of  $\text{Rb}_3\text{V}_5\text{O}_{14}$ , *J. Solid State Chem.* 183 (2010) 2759–2762.
- [15] R.E. Sykora, K.M. Ok, P.S. Halasyamani, D.M. Wells, T.E. Albrecht-Schmitt, New One-Dimensional Vanadyl Iodates: Hydrothermal Preparation, Structures, and NLO Properties of  $\text{A}[\text{VO}_2(\text{IO}_3)_2]$  (A = K, Rb) and  $\text{A}[(\text{VO})_2(\text{IO}_3)_3\text{O}_2]$  (A =  $\text{NH}_4$ , Rb, Cs), *Chem. Mater.* 14 (2002) 2741–2749.
- [16] W.G. Mumme, J.A. Watts, The crystal structure of reduced cesium vanadate,  $\text{CsV}_2\text{O}_5$ , *J. Solid State Chem.* 3 (1971) 319–322.
- [17] Y. Ueda, M. Isobe, Magnetic Properties of  $\text{AV}_2\text{O}_5$  (A = Li, Na, Cs, Ca and Mg) *Journal of Magn. Magn. Mater.* 177–181 (1998) 741–742.
- [18] A single crystals of  $\text{CsV}_2\text{O}_5$  with dimensions of  $0.12 \times 0.09 \times 0.08 \text{ mm}^3$  were isolated from the crushed melted sample, and was mounted on a glass fiber for single crystal X-ray diffraction analyses. Data collection of the complex was performed on a BRUKER SMART CCD Apex II three-circle diffractometer with graphite-monochromated Mo-K $\alpha$  radiation ( $\lambda = 0.71073 \text{ \AA}$ ) at room temperature. All absorption corrections were applied using the SADABS program [19]. Cell refinement and data reduction were carried out with the use of the program SAINT in APEX II [20]. The structure was solved by the direct methods using program SHELXS and refined with the full-matrix least-squares by program SHELXL [21].
- [19] SMART Version 5.054 Data Collection and SAINT-Plus Version 6.45a Data Processing Software for the SMART System, Bruker Analytical X-ray Instruments, Inc, Madison, WI, USA, 2003.
- [20] Bruker, APEX2 Version 2.1–4 and SAINT Version 7.23a Data Collection and Processing Software, Bruker Analytical X-ray Instruments, Inc, Madison, WI, USA, 2006.
- [21] G.M. Sheldrick, *Acta Crystallogr., Sect. A: Found. Crystallogr.* 64 (2008) 112–122.
- [22] S.Q. Kurtz, T.T. Perry, A powder technique for the evaluation of nonlinear optical materials, *J. Appl. Phys.* 39 (1968) 3798–3813.
- [23] J.P. Dougherty, S.K. Kurtz, A second harmonic analyzer for the detection of non-centrosymmetry, *J. Appl. Crystallogr.* 9 (1976) 145–158.